

AD-779 587

ANTENNA DESIGN CONSIDERATIONS FOR A  
HARBOR SURVEILLANCE RADAR

A. J. Core, Jr.

Johns Hopkins University

Prepared for:

U.S. Coast Guard

November 1973

DISTRIBUTED BY:

**NTIS**

National Technical Information Service  
U. S. DEPARTMENT OF COMMERCE  
5285 Port Royal Road, Springfield Va. 22151

# Technical Report Documentation Page

|   |   |  |
|---|---|--|
| 1. Report No.<br>CG-D-58-74   | 2. Government Accession No.   | 3. Recipient's Catalog No.<br>AD 779587  |
| 4. Title and Subtitle<br>Antenna Design Considerations for a Harbor Surveillance Radar  | 5. Report Date<br>November 1973   | 6. Performing Organization Code  |
| 7. Author(s)<br>A. J. Cote, Jr.   | 8. Performing Organization Report No.<br>MSC-73-350   | 10. Work Unit No. (TRAIS)  |
| 9. Performing Organization Name and Address<br>The Johns Hopkins University Applied Physics Lab.<br>8621 Georgia Ave.<br>Silver Spring, Md. 20910   | 11. Contract or Grant No.   | 13. Type of Report and Period Covered<br>FINAL REPORT,<br>February-November 1972 |
| 12. Sponsoring Agency Name and Address<br>Commandant<br>U.S. Coast Guard Headquarters<br>400 Seventh St., N. W.<br>Washington, D. C. 20590  | 14. Sponsoring Agency Code  |  |
| 15. Supplementary Notes   |   |  |
| 16. Abstract<br>This report describes the examination of antenna design parameters performed during early development activity on the San Francisco Experimental Vessel Traffic System. This report outlines the basis for the initial choice of the antenna specifications; the final specifications varied slightly from those listed herein. |   |  |
| <p>Reproduced by<br/>NATIONAL TECHNICAL<br/>INFORMATION SERVICE<br/>U S Department of Commerce<br/>Springfield VA 22151</p>   |   |  |
| 17. Key Words<br>ANTENNA DESIGN<br>VESSEL TRAFFIC SYSTEM<br>SEA CLUTTER   | 18. Distribution Statement<br>This document is available to the public through the National Technical Information Service, Springfield, Va. 22151 |  |
| 19. Security Classif. (of this report)<br>UNCLASSIFIED  | 20. Security Classif. (of this page)<br>UNCLASSIFIED  | 21. No. of Pages<br>34   |
|   |   | 22. Price<br>325   |

UNITED STATES COAST GUARD  
ENVIRONMENTAL AND TRANSPORTATION  
TECHNOLOGY DIVISION REPORT

ANTENNA DESIGN CONSIDERATIONS FOR  
A HARBOR SURVEILLANCE RADAR

by A. J. Cote, Jr.

THE JOHNS HOPKINS UNIVERSITY APPLIED PHYSICS  
LABORATORY  
SILVER SPRING, MARYLAND

This document is disseminated under the sponsorship of the Department of Transportation in the interest of information exchange. The United States Government assumes no liability for its contents or use thereof.

The contents of this report do not necessarily reflect the official view or policy of the Coast Guard, and they do not constitute a standard, specification, or regulation.

This report, or portions thereof, may not be used for advertising, publication, or promotional purposes. Citation of trade names and manufacturers does not constitute endorsement or approval of such products.



W. E. LEHR  
Commander, U. S. Coast Guard  
Chief, Environmental and  
Transportation Technology Division  
Office of Research and Development  
U. S. Coast Guard Headquarters  
Washington, D. C. 20590

## CONTENTS

|    |                       |   |   |   |    |
|----|-----------------------|---|---|---|----|
|    | List of Illustrations | . | . | . | v  |
| 1. | Introduction          | . | . | . | 1  |
| 2. | Radar Resolution      | . | . | . | 3  |
| 3. | Sea Clutter           | . | . | . | 7  |
| 4. | Precipitation Clutter | . | . | . | 17 |
| 5. | Other Considerations  | . | . | . | 27 |
|    | Appendixes            |   |   |   |    |
| A. | References            | . | . | . | 29 |
| B. | CPS Software          | . | . | . | 31 |

## ILLUSTRATIONS

|    |  |    |
|----|--|----|
| 1  | Entrance to Oakland Inner Harbor . . .   | 4  |
| 2  | Richmond Area . . .  | 5  |
| 3  | Point Bonita Area . . .  | 8  |
| 4  | X-Band Sea Backscatter Coefficient,<br>Horizontal Polarization . . .             | 9  |
| 5  | X-Band Sea Backscatter Coefficient,<br>Vertical Polarization . . .               | 10 |
| 6  | S-Band Sea Backscatter Coefficient . . .   | 11 |
| 7  | Impact of Antenna Polarization for Equal<br>Signal-to-Clutter Ratios . . .       | 13 |
| 8  | Impact of Antenna Polarization Assuming<br>Different Clutter Distributions . . . | 14 |
| 9  | Influence of Vertical Beamwidth on<br>Minimum Range, Point Bonita . . .          | 18 |
| 10 | Influence of Vertical Beamwidth on<br>Minimum Range, Yerba Buena Island . . .    | 19 |
| 11 | Effect of Precipitation Clutter at Point<br>Bonita . . .                         | 21 |
| 12 | Effect of Precipitation Clutter at Yerba<br>Buena Island . . .                   | 22 |
| 13 | Yerba Buena Antenna Options . . .  | 23 |
| 14 | Point Bonita Antenna Options . . .   | 24 |
| 15 | Precipitation Clutter at Point Bonita . . .                                      | 25 |
| 16 | Precipitation Clutter at Yerba Buena . . .                                       | 26 |

## 1. INTRODUCTION

To minimize clutter problems and resolve contacts in close proximity, harbor surveillance radars should use high resolution antennas. The influence of these considerations on the choice of parameters desired for the two radars eventually installed in the San Francisco Experimental Vessel Traffic System was examined during the early development activity. Although the antenna specifications projected at that time differed somewhat from those finally used, the Coast Guard has requested that the basis for the original specifications be documented; that is the intent of this report.

It will be seen that clutter considerations dominated the design of the antenna for the Point Bonita site while resolution was the essential constraint on the Yerba Buena Island antenna.

## 2. RADAR RESOLUTION

Three sections of the Yerba Buena Island (YBI) surveillance area place restrictions on resolution: the entrance to the Oakland Inner Harbor and two channels near Richmond (Ref. 1).

In the former case (Fig. 1, extending radially at about 4 o'clock), the junction of the Inner Harbor Entrance Channel and the Inner Harbor Reach narrows to 500 feet at a point 1.9 nmi from the YBI antenna. Since this channel is approximately parallel to the radar line of sight, cross-channel discrimination must be accomplished via antenna azimuth resolution. To split this width into quarters, the required beamwidth is:

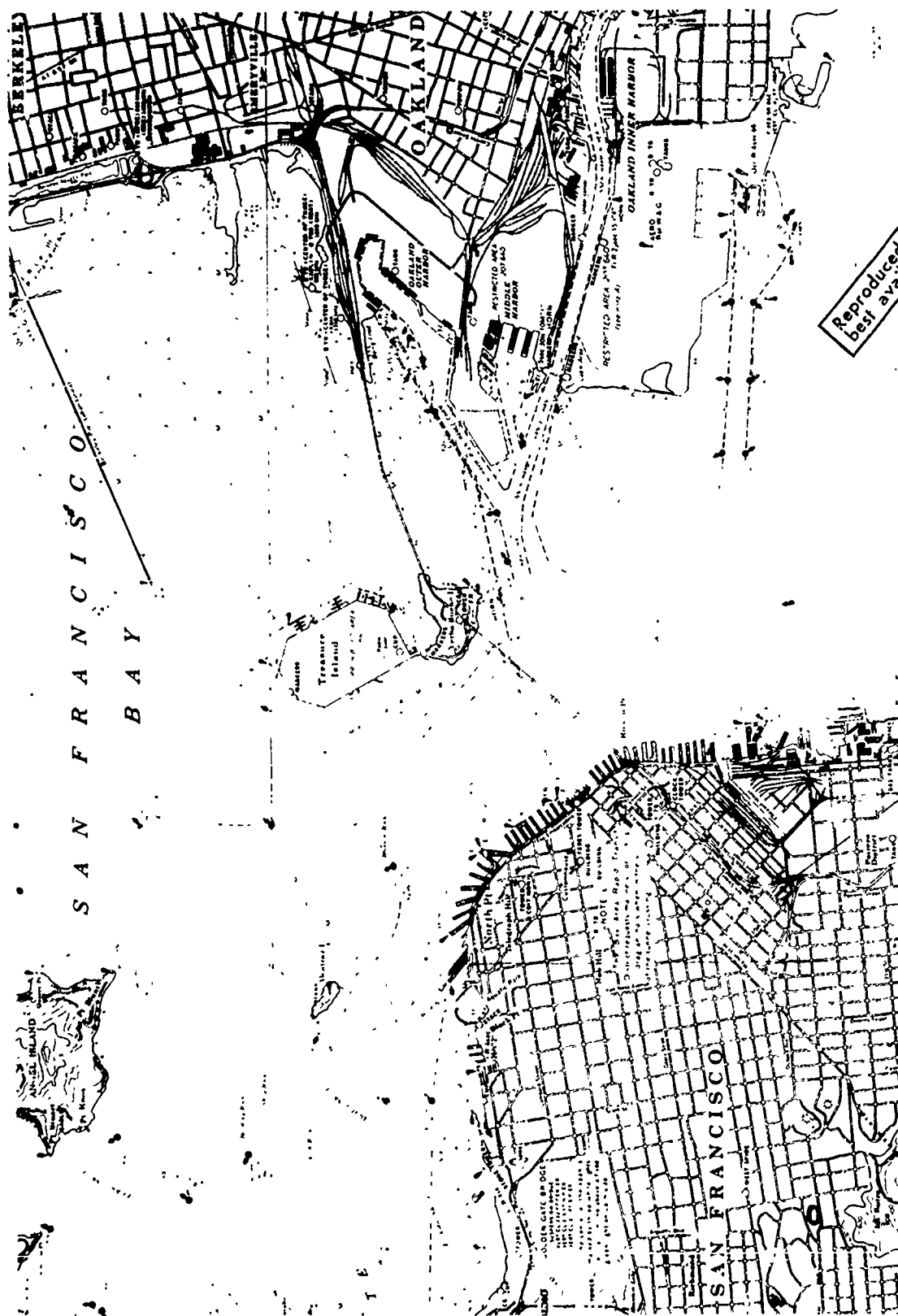
$$\begin{aligned}\theta_{OJ} &= \tan^{-1} \frac{500}{4 \cdot 1.9 \cdot 6076} \\ &= 0.620^\circ.\end{aligned}$$

At the start of the bend further into the reach, the channel width is still only 600 feet; however, the distance from the radar has increased to 3.25 nmi, and the resolution requirement is more stringent:

$$\begin{aligned}\theta_{OB} &= \tan^{-1} \frac{600}{4 \cdot 3.25 \cdot 6076} \\ &= 0.435^\circ.\end{aligned}$$

In the Richmond area (Fig. 2), there are two channels of interest. The Point Potrero Reach is 500 to 600 feet wide, but it is essentially perpendicular to the YBI radial, and cross-channel discrimination can be achieved through use of a narrow radar pulse width. The northern end of the Southampton Shoal Channel (11 o'clock radial) is 600 feet wide, 7.2 nmi from the YBI site, and parallel to the radar radial. It requires an azimuth beamwidth of:

$$\begin{aligned}\theta_{SH} &= \tan^{-1} \frac{600}{4 \cdot 7.2 \cdot 6076} \\ &= 0.196^\circ.\end{aligned}$$



Reproduced from  
best available copy.

Fig. 1 ENTRANCE TO OAKLAND INNER HARBOR



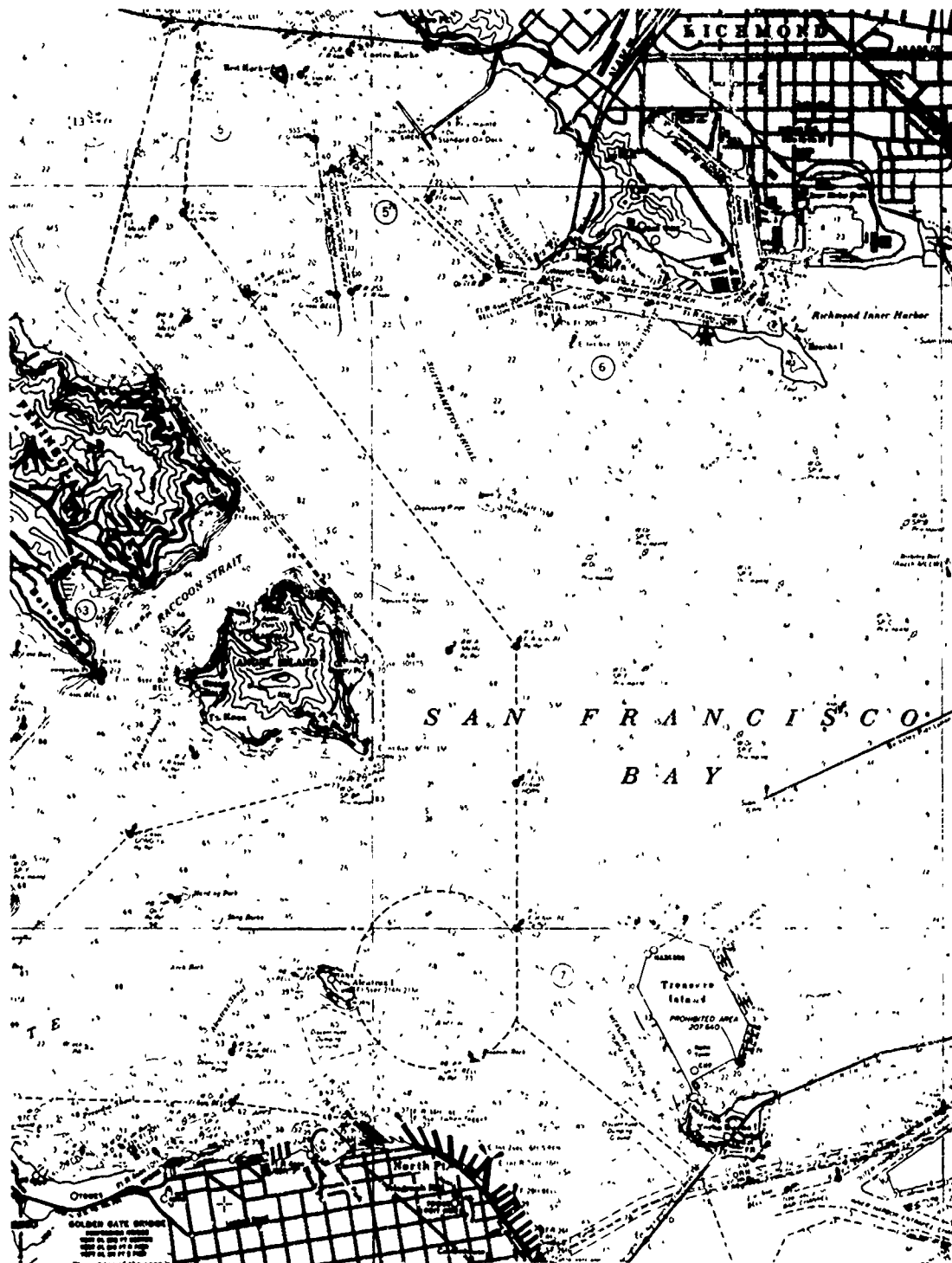


Fig. 2 RICHMOND AREA

Based only on these considerations, the Southampton constraint would define the azimuth beamwidth requirement for the YF1 radar. However, the Coast Guard indicated that the Oakland Inner Harbor Reach should be the basis for setting the azimuth specification on the grounds that another radar is likely to be placed at Richmond if the system is ever expanded. To resolve the Southampton Shoal Channel, the Automatic Detection and Tracking portions of the San Francisco system use data received on successive dwells to determine the centroid of a contact, thus achieving discrimination between contacts separated by less than the beamwidth.

### 3. SEA CLUTTER

Since the Point Bonita radar looks primarily seaward (Fig. 3), resolution is significant only in separating targets. The 2000 foot wide Main Ship Channel is more easily resolved than the Oakland Inner Harbor Reach, even though its distant end is 5.8 nmi from the Point Bonita site. Sea clutter dominates the design of this antenna. A pulse radar viewing sea clutter at low grazing angles has a maximum range given (Ref. 2) by:

$$R_{\max} = \frac{2 \sigma \cos \phi}{(s/c) \sigma_o \theta c \tau}$$

where:

- $\sigma$  = target cross section,
- $\phi$  = grazing angle,
- $s/c$  = minimum signal-to-clutter ratio,
- $\sigma_o$  = sea backscatter coefficient,
- $\theta$  = antenna azimuth beamwidth,
- $c$  = velocity of propagation, and
- $\tau$  = radar pulse width.

This equation can be employed to estimate the detectable contact cross section as a function of range and sea state. However, there are a number of assumptions which influence the result, and they warrant discussion.

The first problem is to obtain usable values from the backscatter coefficient. We have employed those of Ref. 3 to generate Figs. 4, 5, and 6. The tables from which the data points were obtained were compiled using experimental data from numerous sources. Assumptions and constraints are summarized in the reference. For our purposes, the most serious of these appears to be that the data was based on pulse lengths in the 0.5 to 10  $\mu$ s region with echoes having approximately Rayleigh distributions. But the VTS radars will have 50 ns transmitters so that clutter distribution can be expected to depart from that model.

Despite this limitation, the data has been employed in the hope that it offers some guidance in the selection of at

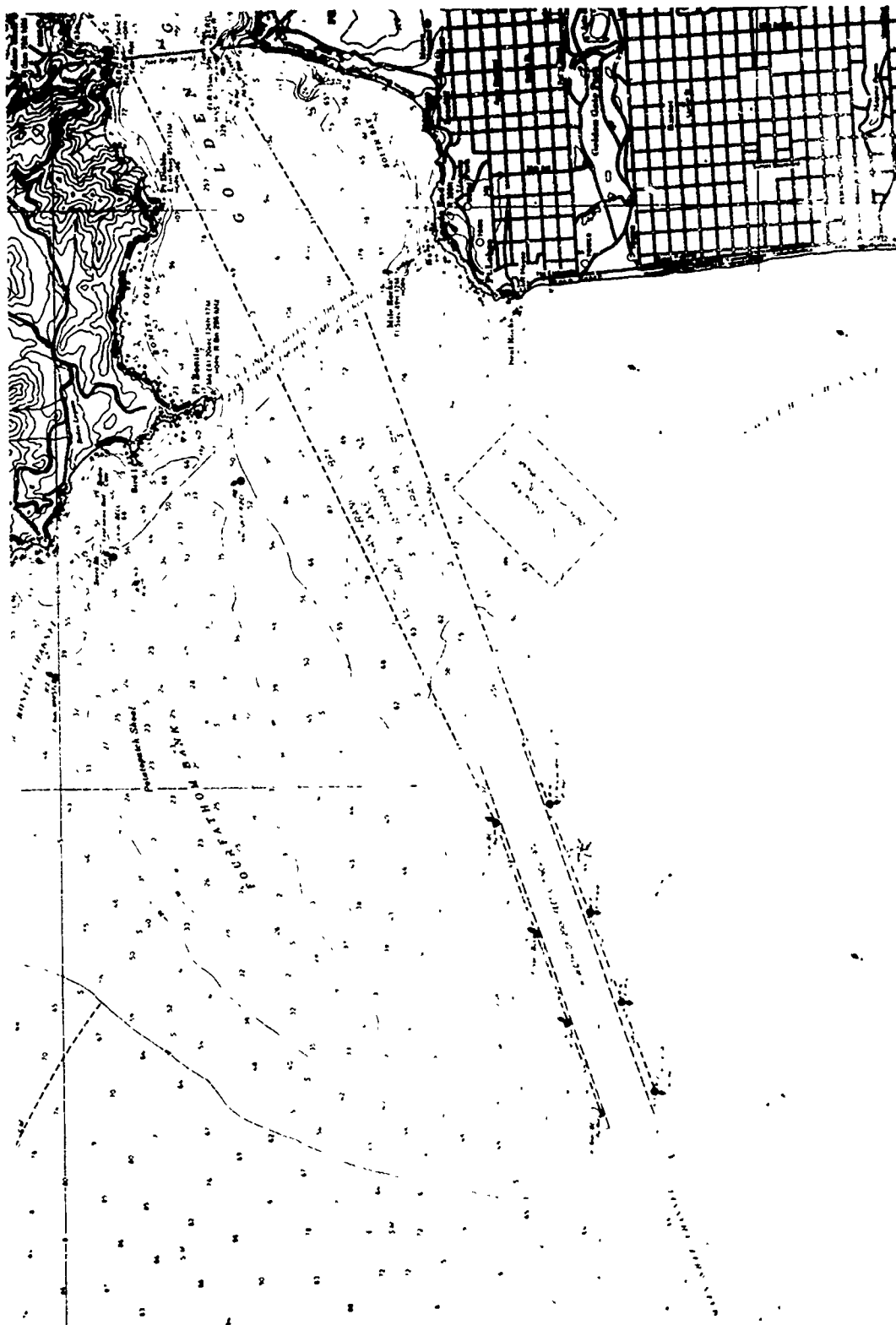


Fig. 3 POINT BONITA AREA

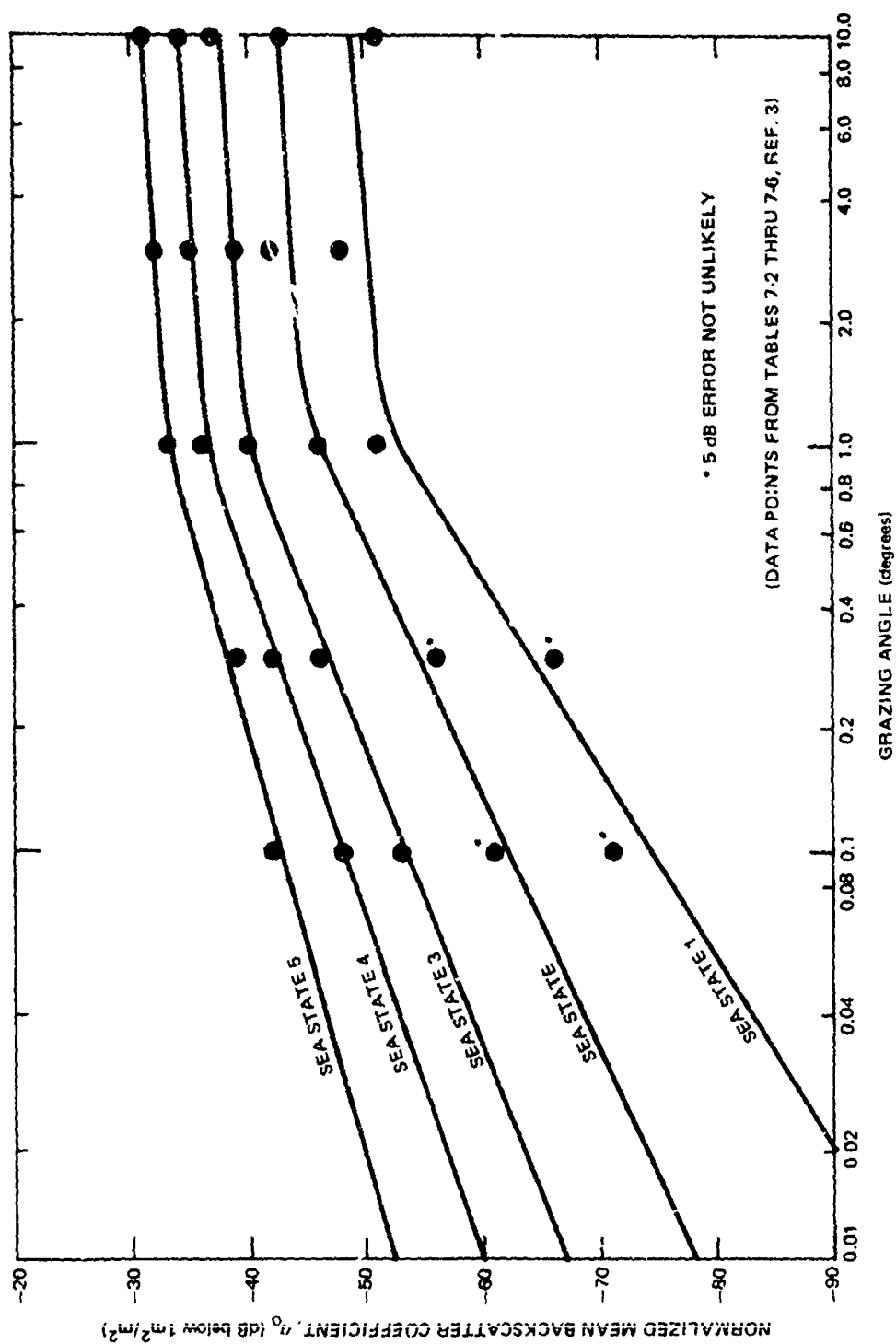


Fig. 4. X-BAND SEA BACKSCATTER COEFFICIENT, HORIZONTAL POLARIZATION

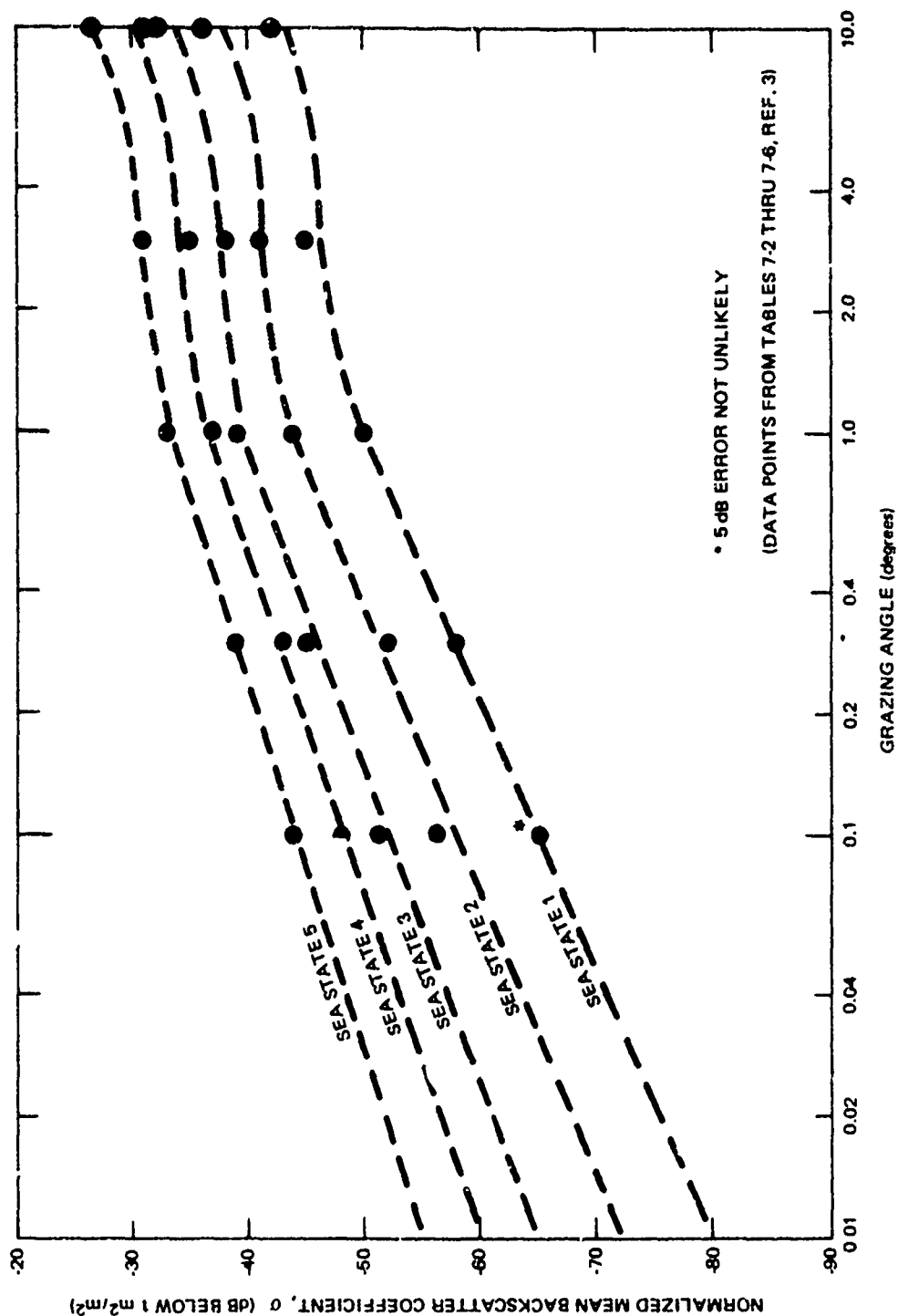


Fig. 5. X-BAND SEA BACKSCATTER COEFFICIENT, VERTICAL POLARIZATION

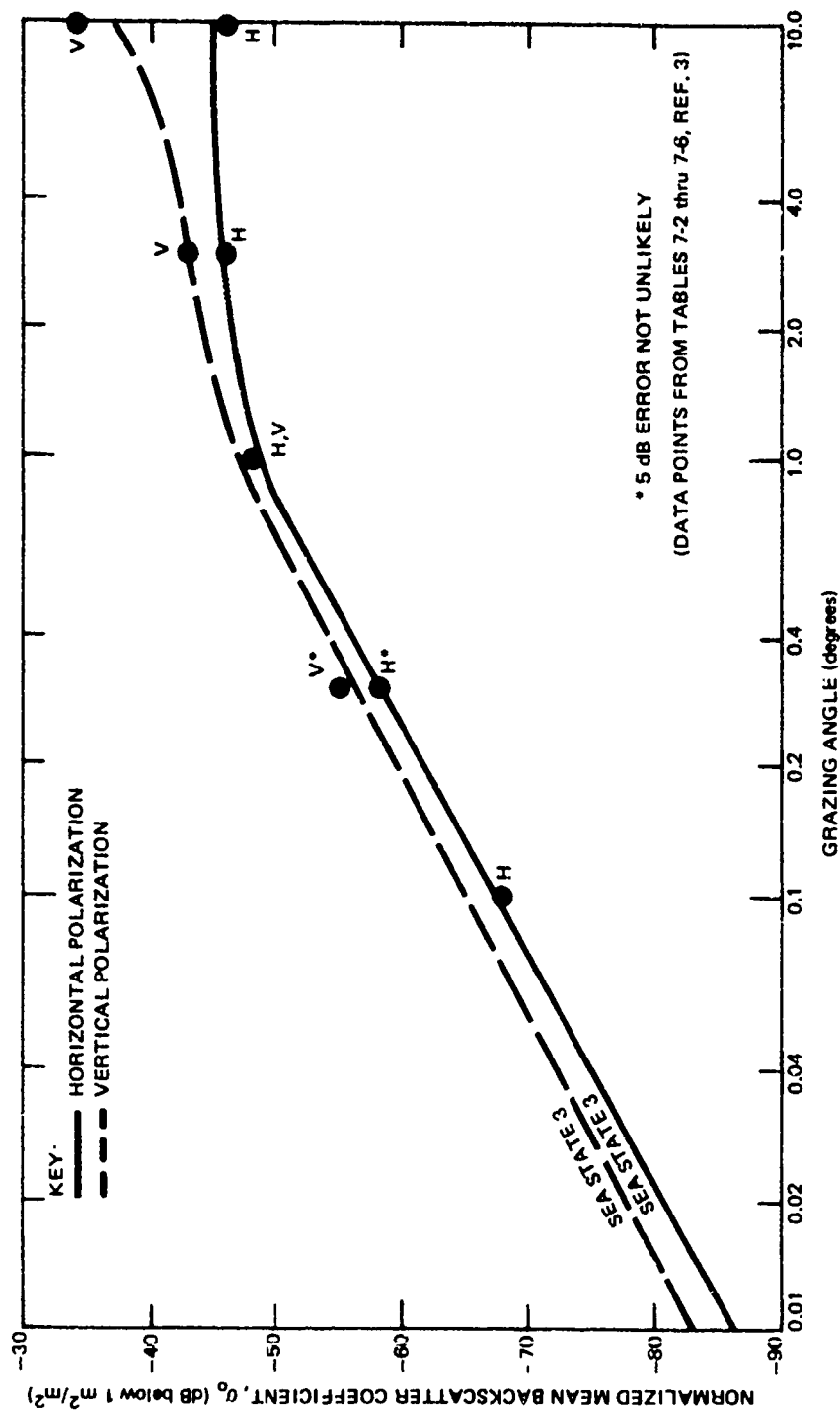


Fig. 6. S-BAND SEA BACKSCATTER COEFFICIENT

least antenna polarization. For example, consider Fig. 7. Antenna beamwidth was set as narrow as seemed practical (i.e.,  $0.25^\circ$ ) on the grounds that it is comparable to that employed in some of the European harbor radars and leads to a not unreasonable aperture on the order of 30 feet. Assuming a 16 dB signal-to-clutter ratio is required to prevent false alarm overload of the radar computer, the detectable contact cross sections are as shown for the two polarizations. Although not plotted, horizontal polarization offered an even further advantage over vertical at sea state 1. For example, at 3 nmi, the detectable cross sections were 0.029 and 0.63  $\text{m}^2$  respectively. Thus, it appears that horizontal polarization might be the better choice.

However, the literature also offers evidence that, as pulse lengths decrease, the departure from Rayleigh is greater for horizontal polarization than for vertical (Refs. 2 through 5). This might prove significant enough to offset an apparent horizontal polarization advantage for the following reasons.

The requirement to minimize radar computer saturation sets a value for false alarm rate. In this application, it is on the order of  $10^{-5}$ . Assume we require a 0.5 probability of detection and are unable to obtain the benefits of pulse-to-pulse integration (e.g., because of the high resolution and long correlation time). If vertical polarization yields Rayleigh statistics, the required s/c ratio is 10 dB for  $n = 1$ . If horizontal polarization results in log-normal returns, then to achieve the same false alarm rate, the s/c value must be much greater (e.g., 26 dB for sea state 3). Given such assumptions, the resulting difference in detectable contact cross section is shown in Fig. 8.

One might legitimately challenge the specific numerical difference noted in the figure on grounds that:

1. Backscatter coefficients were not defined at short pulses and are thus suspect to some extent, and
2. Vertical polarization has some log-normal tendencies rather than being pure Rayleigh as assumed in arriving at that result.



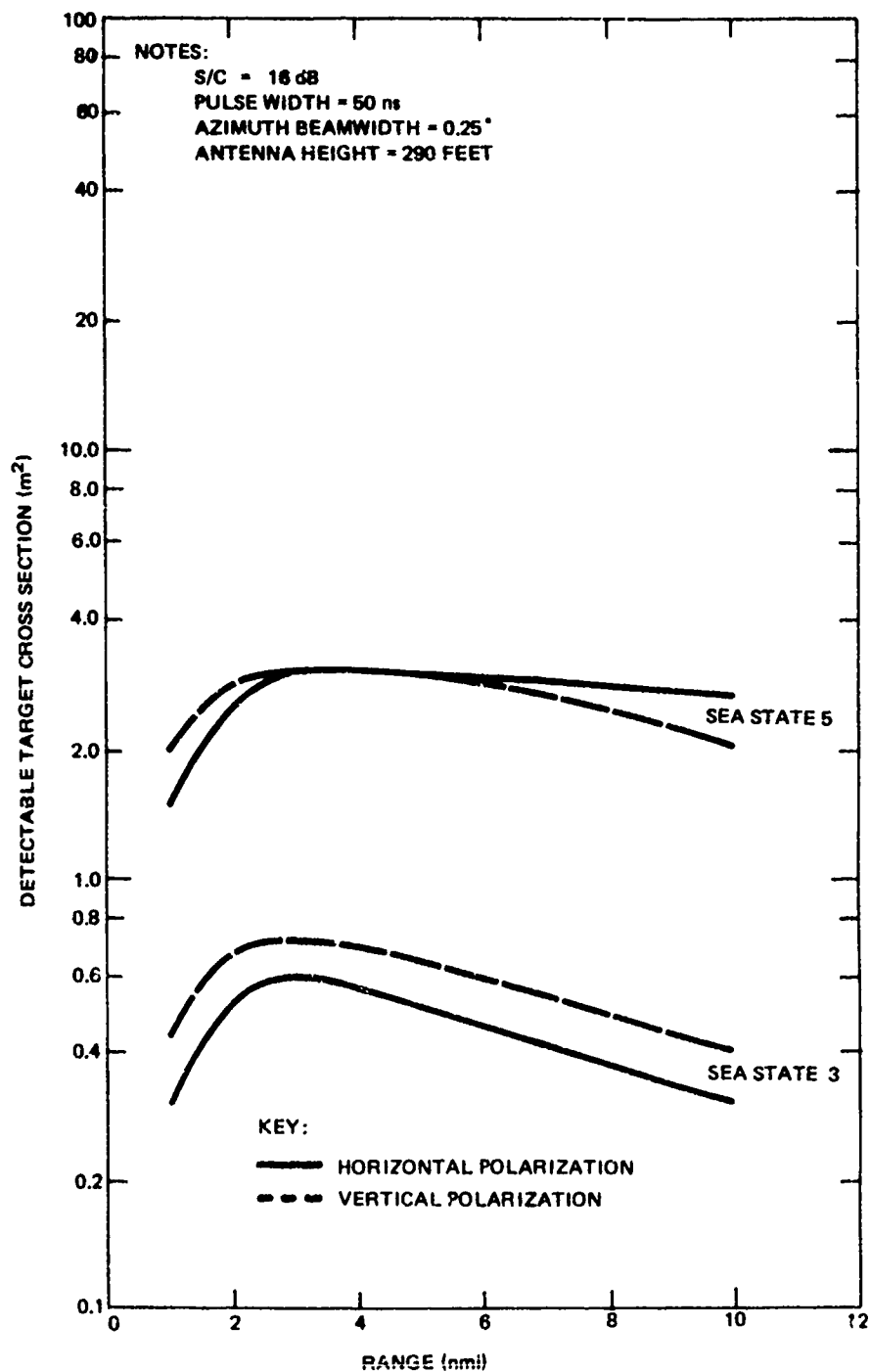


Fig. 7. IMPACT OF ANTENNA POLARIZATION FOR EQUAL SIGN/ L-TO-CLUTTER RATIOS

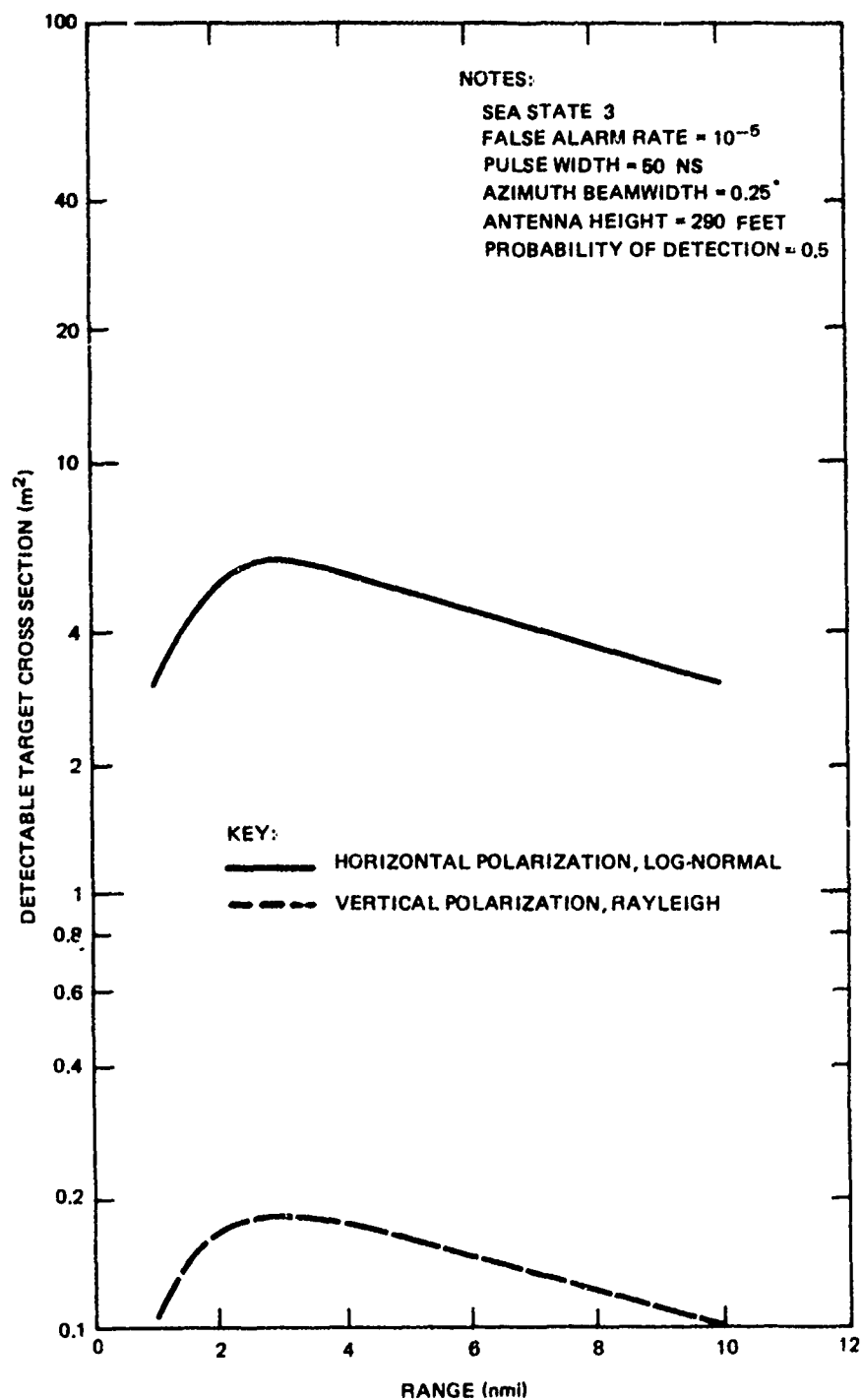


Fig. 8. IMPACT OF ANTENNA POLARIZATION ASSUMING  
DIFFERENT CLUTTER DISTRIBUTIONS

However, the literature does offer support for the difference in distributions. At higher sea states, the advantage should be further in favor of vertical; with calmer waters, the advantage would decline or even vanish. However, at the lower sea states, small contact detection is not as great a problem.

Thus we conclude that the Point Bonita antenna should use vertical polarization. For the calmer conditions encountered within the harbor, horizontal polarization is perhaps the better choice, since the calmer waters (in which horizontal polarization has an advantage) will occur a greater portion of the time than it will for the Point Bonita surveillance area.

If the absolute values in either Fig. 7 or 8 are accurate, one could argue that the narrow azimuth beamwidth constitutes an overkill and a smaller aperture antenna could be deployed for Point Bonita at less expense. But the many uncertainties associated with generation of the curves argues for the more prudent approach: an azimuth beamwidth on the order of  $0.25^\circ$ . The YBI azimuth beamwidth was dictated by resolution considerations as  $0.44^\circ$ .

In light of experience at the latter site with rip tides, vertical (rather than horizontal) polarization would probably have been a better choice, although we have no clear cut means of demonstrating that vertical would yield the same advantages it offers against conventional sea clutter.

#### 4. PRECIPITATION CLUTTER

Elevation beamwidths for both radars are determined by requirements for performance in a precipitation environment and surveillance coverage close to the radar sites. We will consider the close-in coverage first. Coverage is required to within about 1200 feet of both the PB and YBI radars. To determine the vertical beamwidth, we first assume a Gaussian-shaped antenna pattern (Ref. 6) given as:

$$f(\alpha) = \exp(-2.88 \frac{\alpha^2}{\phi}) ,$$

where  $\phi$  = the 3 dB vertical beamwidth  
 $\alpha$  = the angle off axis.

The boresight of the antenna is depressed such that the beam illuminates a point at maximum range on a 4/3 earth. From Ref. 3, this is:

$$\beta = \sin^{-1}(\frac{h}{R} + \frac{R}{2r_e}) ,$$

where:

$h$  = antenna height  
 $R$  = slant range, and  
 $r_e$  = 4/3 radius of the earth (4587).

Signal strength is inversely proportional to the fourth power of range. Thus, for any given beamwidth, antenna height, and maximum range (290 feet and 15 nmi for PB, 400 feet and 8 nmi for YBI), one can estimate, as a function of range, the signal strength relative to that at maximum range. This is plotted for the two radar sites in Figs. 9 and 10. To achieve the same signal strength at 1200 feet that is available at maximum range, the curves indicate that the vertical beamwidth for the Point Bonita antenna should be approximately 8°. To intercept the surface at maximum range, the boresight should be depressed 0.27°. For Yerba Buena Island, the corresponding angles are 11° and 0.52°, respectively.

These elevation beamwidths combine with the azimuth beamwidth and pulse width to define a volume in space which influences the level of precipitation clutter return. As a

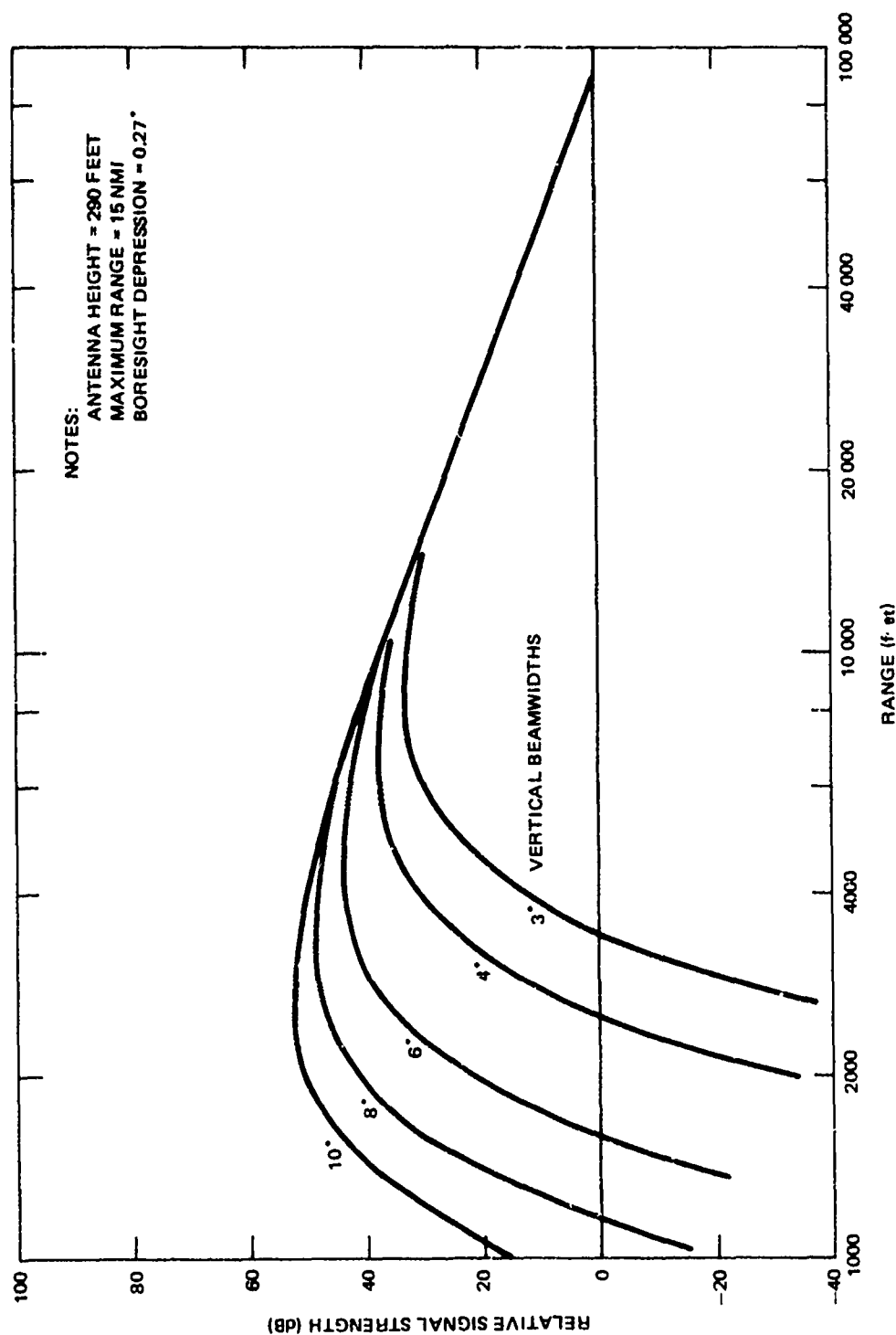


Fig. 9. INFLUENCE OF VERTICAL BEAMWIDTH ON MINIMUM RANGE, POINT EONITA

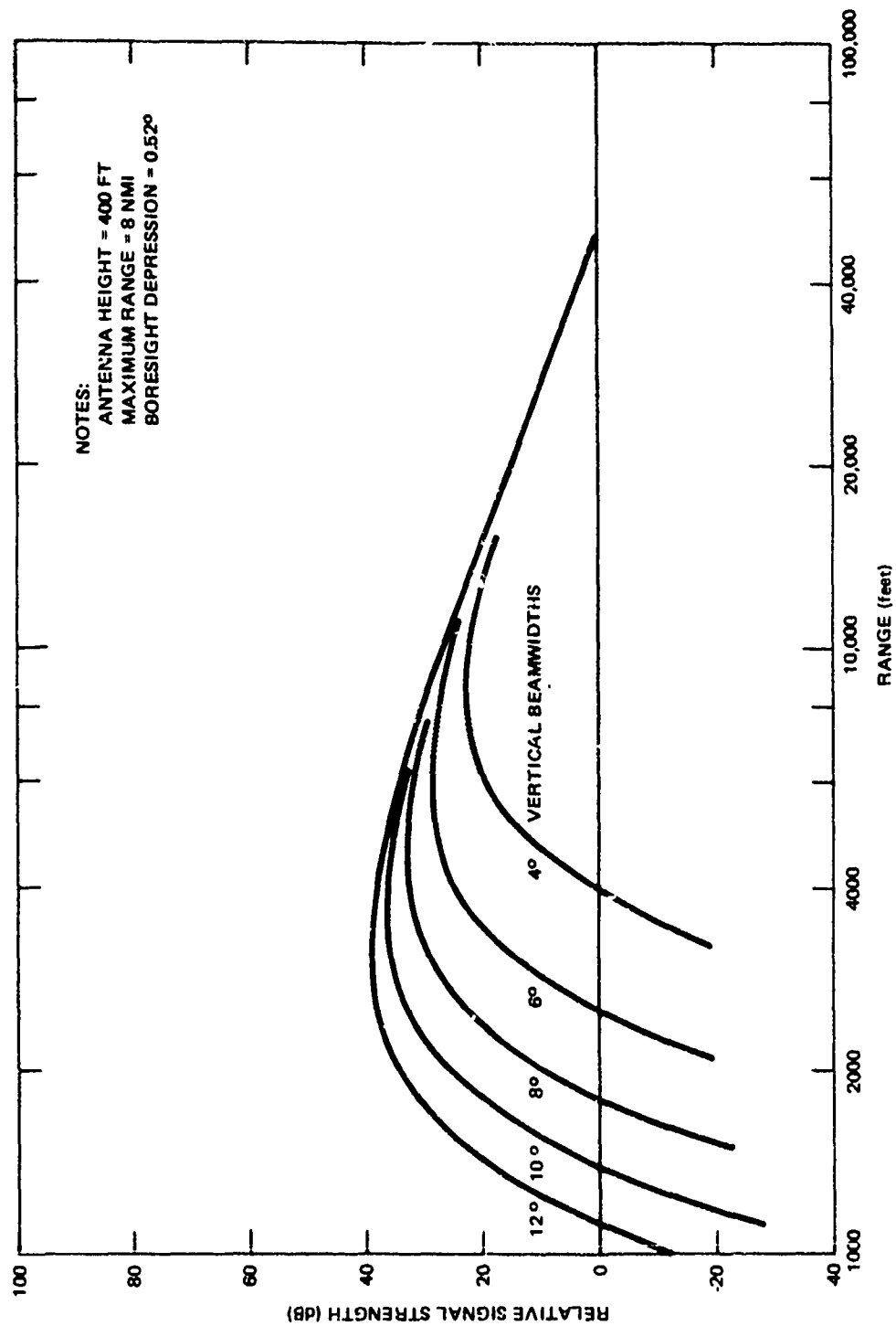


Fig. 10. INFLUENCE OF VERTICAL BEAMWIDTH ON MINIMUM RANGE, YERBA BUENA ISLAND

result, the detectable contact cross section is given approximately by Ref. 3 as:

$$\sigma = R^2 (\pi/8) \theta \phi c \tau (s/c)$$

where:

- R = range,
- $\theta$  = azimuth beamwidth,
- $\phi$  = elevation beamwidth
- c = propagation velocity,
- $\tau$  = pulse width,
- s/c = minimum signal-to-clutter ratio, and
- $\Sigma$  = precipitation backscatter coefficient.

Applying this equation using backscatter coefficients of Ref. 3 yields the performance for the two radars as shown in Figs. 11 and 12.

The solid curves are for linearly polarized antennas and they indicate that either moderate or heavy rain can restrict the detection of 2 m<sup>2</sup> targets. To overcome this limitation, it will be necessary to include provisions for selecting circular polarization on both antennas at the operator's option. Alternately, one could consider decreasing the vertical beamwidth and sacrificing close-in coverage. But the full 13 dB improvement obtainable with circular polarization cannot be matched without a drastic reduction in the vertical beamwidth.

Figures 13 through 16 offer performance projections for relaxed azimuth beamwidths.

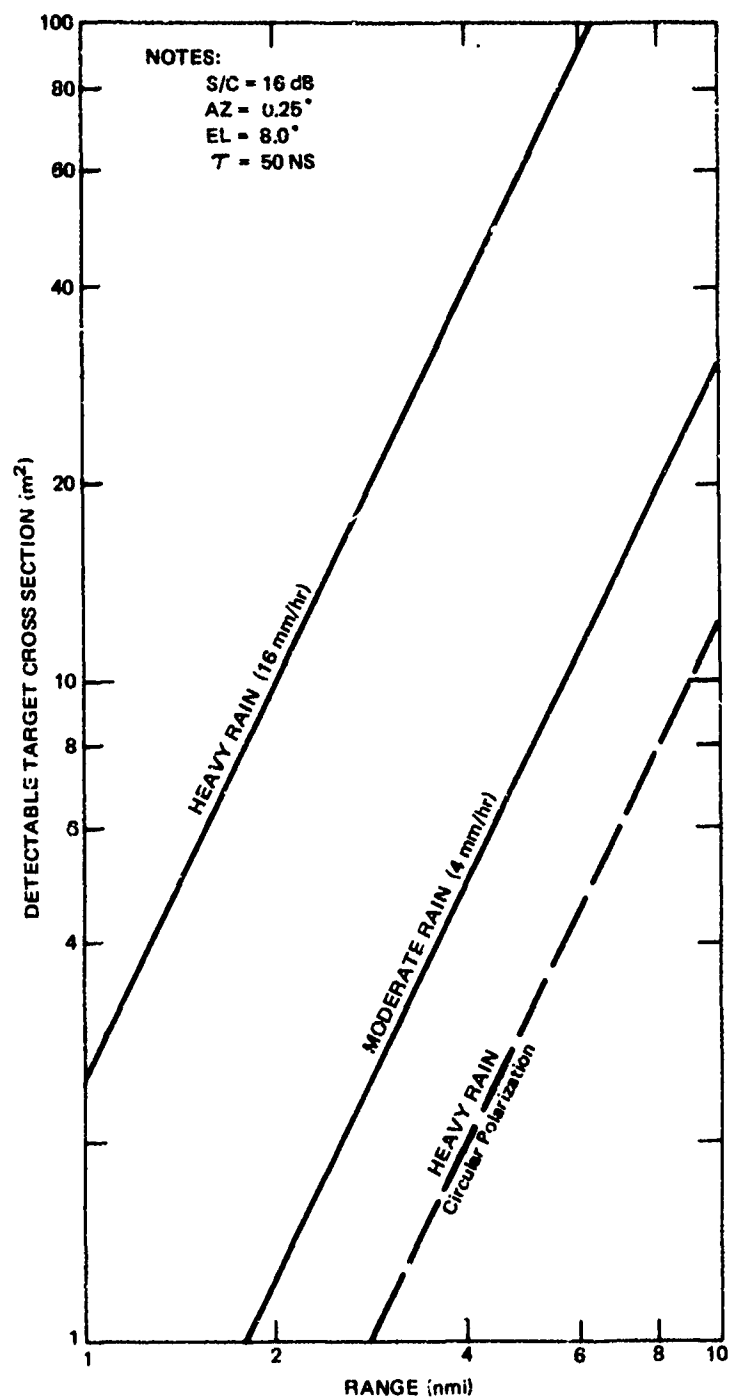


Fig. 11. EFFECT OF PRECIPITATION CLUTTER AT POINT BONITA



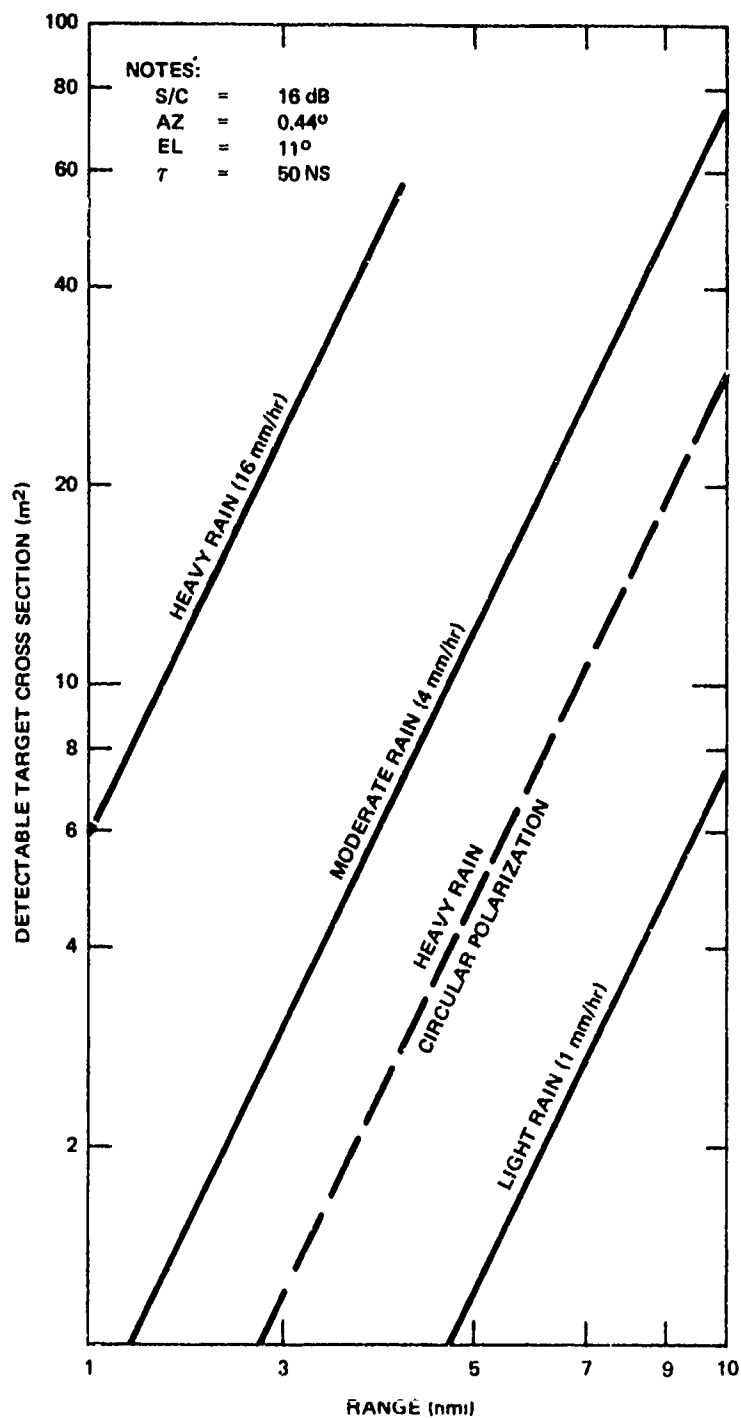


Fig. 12. EFFECT OF PRECIPITATION AT YERBA BUENA ISLAND

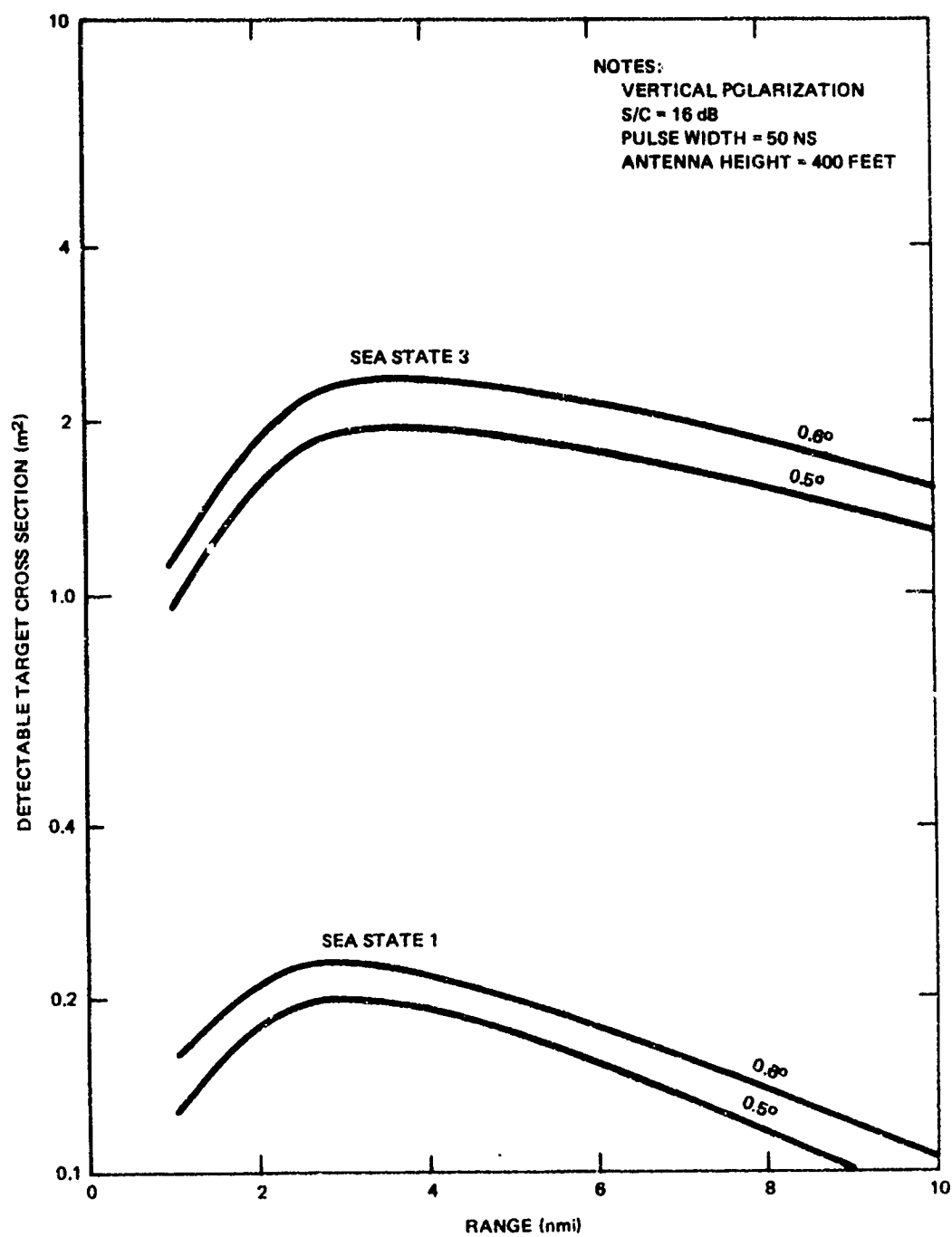


Fig. 13. YERBA BUENA ANTENNA OPTIONS

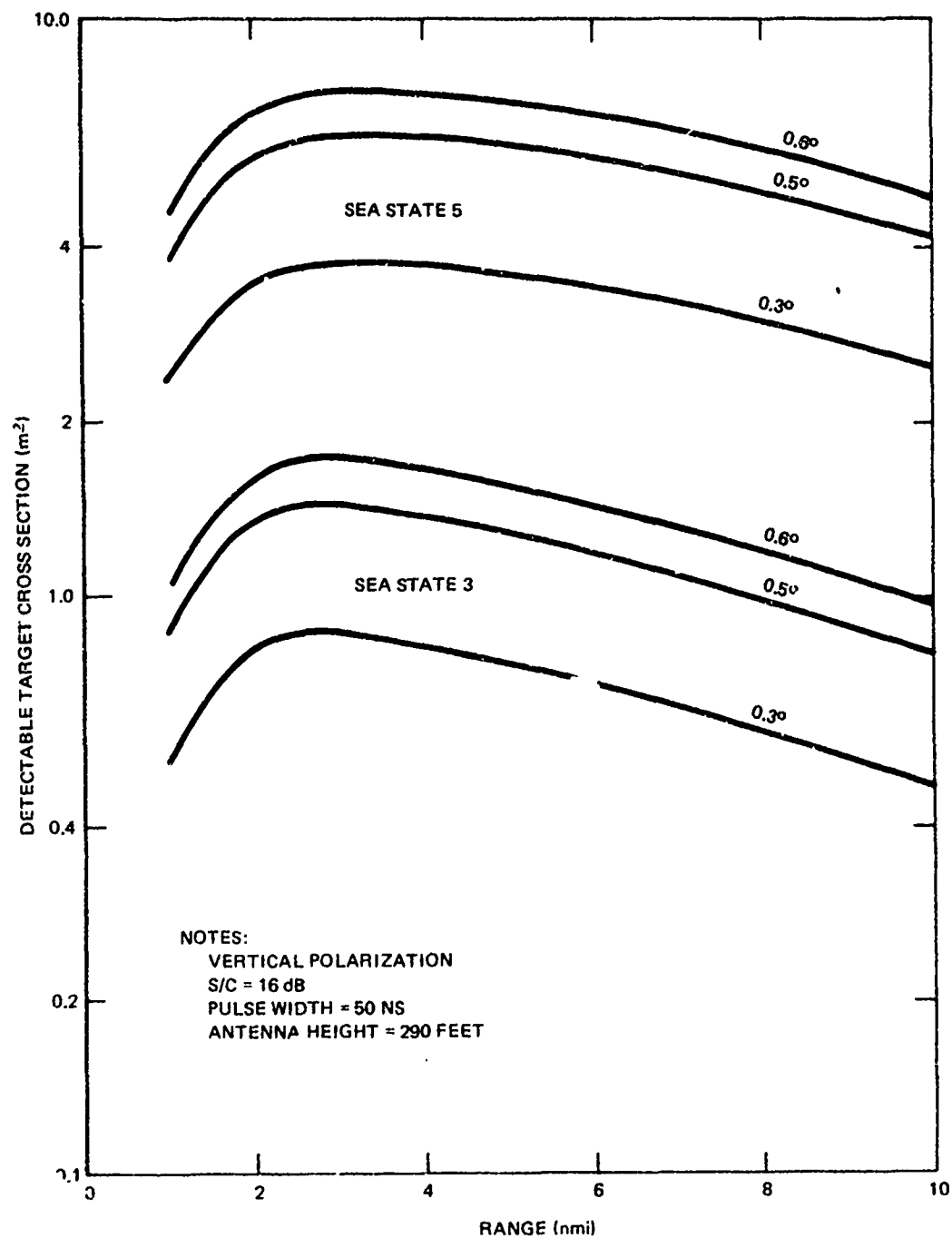


Fig. 14. POINT BONITA ANTENNA OPTIONS



- 25 -

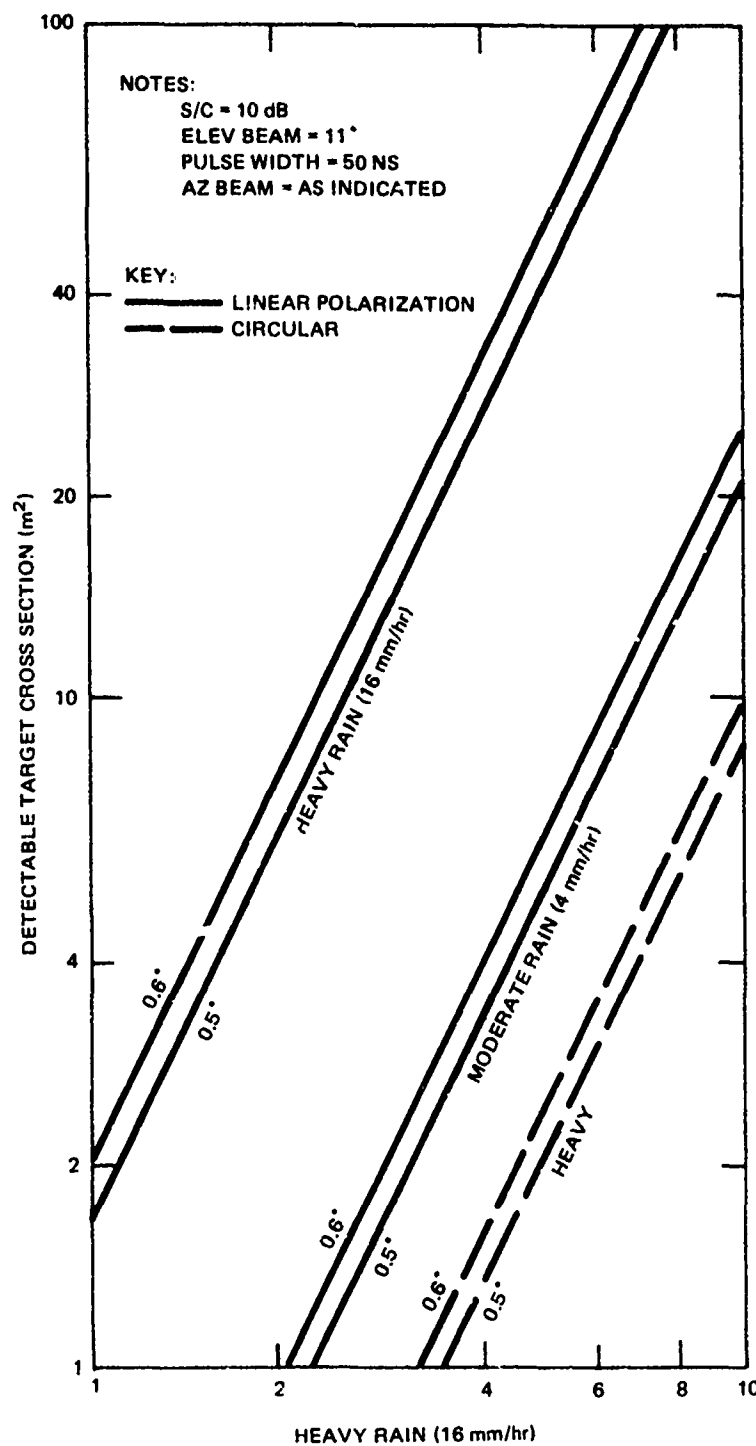


Fig. 16. PRECIPITATION CLUTTER AT YERBA BUENA

## 5. OTHER CONSIDERATIONS

Another aspect to be considered in this antenna design is the effect of lobing on the detection of surface contacts. The elevation angle of the first lobe is approximately  $\lambda/(4h_a)$ , where  $\lambda$  is the wavelength and  $h_a$  is the antenna height (Ref. 5). For the Point Bonita antenna and X-band operation, this is  $(0.031 \cdot 3.281)/(4 \cdot 290) = 8.5 \cdot 10^{-5}$  radians ( $\approx 0.005^\circ$ ). There is a distance at which the free space range dependence shifts to an  $R^{-8}$  dependence given approximately as  $(4h_a h_t)/\lambda$ , where  $h_t$  is the contact height (Ref. 3). Again, for Point Bonita and X-band, assuming a 3 foot contact height, this range is

$$(4 \cdot 290 \cdot 3)/(0.031 \cdot 3.28) = 34\,200 \text{ feet,}$$

or 5.6 nmi. For this same antenna and S-band operation, the angle and range are  $0.005 \cdot 10/3.1 = 0.016^\circ$  and  $5.6 \cdot 3.1/10 = 1.73$  nmi, respectively. This last result tends to make S-band operation less attractive than X-band because of its impact on power requirements. For the YBI radar, with its 400 foot antenna height, the X-band transition range is  $5.6 \cdot 400/290 = 7.7$  nmi.

The distance in nautical miles to the radar horizon, assuming a 4/3 earth, is  $1.23 h_a$ , where  $h_a$  is in feet (Ref. 4). For X-band operations, the horizon is 21.0 nmi and 24.6 nmi for PTB and YBI respectively.

Finally, consideration was also given to use of an inverse cosecant squared vertical beam pattern as a means of achieving close-in coverage and obtaining a constant received signal independent of range. The possibility has not been entirely discarded but since a loss in gain would result and the broadened beam would adversely affect precipitation performance, a decision has been deferred pending determination of the remaining radar parameters.\*

The CPS software employed in the calculation is included as Appendix A to this report.

---

\*The final antenna design did, in fact, approximate the cosecant squared vertical pattern through the use of a secondary feed.

## APPENDIX A

### REFERENCES

1. "Entrance to San Francisco Bay," Coast and Geodetic Survey C and GS Chart 5532, 23 May 1970.
2. M. J. Skolnik (ed), Radar Handbook, McGraw-Hill, 1970.
3. F. E. Nathanson, Radar Design Principles, McGraw-Hill, 1969.
4. G. V. Trunk and S. F. George, "Detection of Targets in Non-Gaussian Sea Clutter," IEEE Trans. Aerospace and Electronic Systems, Vol. AES-6, September 1970, pp. 620-628.
5. M. I. Skolnik, Introduction to Radar Systems, McGraw-Hill, 1962, p. 503.
6. ITT, "Reference Data for Radio Engineers," Howard Sams and Co., 1968.

## APPENDIX B

### CPS SOFTWARE

The attached listing is a PL/I program used to expedite some of the calculations associated with creating the figures. It is used at a conversational terminal.

For example, calling CLUT lets the user enter a signal-to-clutter ratio, pulse width, azimuth beamwidth, and antenna height. The program then computes the grazing angle for several preset ranges. The user then uses Fig. 4 or 5 to obtain the backscatter coefficient for each angle and enters that data. The program replies with the resulting detectable target cross-section, thus providing a point for curves like those in Figs. 7 and 8.

The routine PREC will provide data for a figure like Fig. 15 when the user supplies arguments for azimuth angle, elevation angle, pulse width, and signal-to-clutter ratios.



```

10. DBC:  PROCEDURE (a);
12.      c=TRUNC(a/1000);
14.      IF c=0 THEN b=a;
16.      IF c=0 THEN GO TO A; ELSE b=MOD(a,c);
18. A:    e=SIGN(a);
20.      d=10*(ABS(b)/10)+10*c;
22.      IF a>0 THEN RETURN (d);
24.      IF a=0 THEN RETURN (1);
26.      IF a<0 THEN RETURN (1/d);
28.      END DBC;
30. SIGC: PROCEDURE (f,g);
32.      X=g/(f*6076)-f/(2*4587);
34.      PS=ATAN(X,SQRT(1-X**2));
36.      PSD=PS*(180/3.14159);
38.      PUT LIST('R=',f,'nm Psi=',PSD,'degrees');
40.      END SIGC;
42. CLUT: PROCEDURE ;
44.      PUT LIST('S/C ratio (db), Tau (nsec), Az Beam (deg), Ant Ht (ft)');
46.      GET LIST(SCD,TAU,AZD,HF);
48.      SC=DBC(SCD);
50.      TAS=TAU*.1E-08;
52.      AZR=AZD*(3.14159/180);
54.      PUT LIST(' ');
56.      DO R=1,1.5,2,2.5,3,4,6,8,10;
58.      CALL SIGC(R,HF);
60.      PUT LIST('SIGO for that PSI');
62.      GET LIST(SIGO);
64.      SIGR=DBC(SIGO);
66.      SIGTR=R*1852*SIGR*SC*AZR*.3EJ9*.5*TAS/COSD(PSI);
68.      PUT LIST(R,'nm SIGMA=',SIGTR,'sq m');
70.      PUT LIST(' ');
72.      END CLUT;
74. ELAN: PROCEDURE (h,rmax,rmin);
76.      AA=SQRT(h**2+rmin**2);
78.      B=SQRT(h**2+rmax**2);
80.      C=rmax-rmin;
82.      aa=ATAND(h,rmax);
84.      Sc=C*SIND(aa)/AA;
86.      cc=ATAND(Sc,SQRT(1-Sc**2));
88.      PUT LIST('El beam =',cc,'degrees');
90.      dd=ATAND(rmin,h);
92.      ee=90-dd-cc/2;
94.      PUT LIST('Depression angle =',ee,'degrees');
96.      END ELAN;
98. ANT:  PROCEDURE ;
100.     PUT LIST('Max Ground Range (nm), Antenna Ht (ft)');
102.     GET LIST(rmax,h);
104.     rmaf=6076*rmax;
106.     PUT LIST('Beamwidth (degrees)');
108.     GET LIST(THET);
110.     RSMA=SQRT(h**2+rmaf**2);
112.     BE1=h/RSMA*RSMA/(2*4587*6076);
114.     BETA=ATAND(BE1,SQRT(1-BE1**2));
116.     PUT LIST('BETA=',BETA);
118.     DO ALF=0,1,1.5,2,2.5,3,4,6,8,10,15,20;
120.     GAM=ALF+BETA;
122.     aq=1;
124.     bq=-2*4587*6076*SIND(GAM);
126.     cq=2*h*4537*6076;
128.     RSL=.5*(-bq-SQRT(bq**2-4*aq*cq));
130.     GR=SQRT(RSL**2-h**2);
132.     IF ALF=0 THEN SSMR=1/RSL**4;
134.     FG=EXP(-2.88*(ALF**2/THET**2));

```

THE JOHNS HOPKINS UNIVERSITY  
APPLIED PHYSICS LABORATORY  
SILVER SPRING MARYLAND

```

136.      SIGS=1/SSNR*FG*FG*(1/RSL**4);
138.      PUT LIST('ALF=',ALF,'GR=',GR,'SIG=',L10(SIGS),'db');
140.      IF SIGS<.9 THEN GO TO JF;
142.      END ;
144.      JP:  PUT LIST(' ');
146.      END ANT;
148.      LET L10(c)=10*LOG(c)/2.302581;
150.      PREC: PROCEDURE (az,el,pw,sc);
152.      PUT LIST('Outputs are for 1,4,810 nm');
154.      PUT LIST('Fog, driz, lght mod, hvy (-,.25,1,4,16 mm/hr)');
156.      DO ES=-100,-82,-72,-62,-53;
158.      PUT LIST(' ');
160.      DO R=1,4,10;
162.      RM=R*1852;
164.      PI=3.14159;
166.      SICL=RM*RM*PI*.25*az*el*.3E09*1.745*.0001745*.5*pw*.1E-08*DBC(sc)*DBC(ES);
168.      PUT LIST('Clutter=',ES);
170.      PUT LIST('R=',R,'nm, SIG=',SICL,'sq mtrs');
172.      END PREC;

```